




Extending The Life Cycle of Self-Healed Asphalt Pavements with Recycled Additives

Catherine Gamil Shafik ^{1,*} ; Mohamed R. Elshahat ²; Ahmed Abdelghani Mahmoud ³; Abdelzaher E. A. Mostafa ⁴

1. M.Sc., Department of Civil Engineering, Egyptian Russian University, Cairo, Egypt

2. Assistant Professor, Department of Civil Engineering, Egyptian Russian University, Cairo, Egypt

3. Assistant Professor, Department of Civil Engineering, Faculty of Engineering - Mataria, Helwan University, Cairo, Egypt

4. Professor, Department of Civil Engineering, Faculty of Engineering - Mataria, Helwan University, Cairo, Egypt

* Corresponding author: cathrine-gamil@eru.edu.eg

ARTICLE INFO

Article history:

Received: 03 March 2025

Revised: 05 August 2025

Accepted: 17 August 2025

Keywords:

Sustainable Asphalt Pavement;

Self-Healing;

Induction and Microwave

Heating;

Asphalt Pavement Life Cycle;

Maintenance and Repair Cost.

ABSTRACT

Asphalt is the most used material for constructing road pavements worldwide. However, a major issue that affects asphalt pavement performance and service life is cracking, which is primarily caused by factors such as load and temperature. This paper aims to develop a sustainable asphalt road pavement through the self-healing technique using induction and microwave heating with additives such as electric arc furnace slag (EAFS) and steel wool fiber (SWF). Marshall Stability, Volumetric Properties, Indirect Tensile Strength, moisture resistance, low-temperature cracking resistance, and thermal distribution were studied. The healing index was utilized as an indicator for improving the self-healing of asphalt mixtures. The pavement life cycle was also predicted, and the construction cost was analyzed. The results showed that using EAFS or SWF in the asphalt mixture resulted in significant time and energy consumption. The replacement of natural coarse aggregate with 20% EAFS and/or the addition of 0.2% SWF by weight of the asphalt mixture showed promising results in improving mechanical properties, promoting sustainability, and increasing the pavement life cycle by a percentage up to 47%.

E-ISSN: 2345-4423

© 2025 The Authors. Journal of Rehabilitation in Civil Engineering published by Semnan University Press.

This is an open access article under the CC-BY 4.0 license. (<https://creativecommons.org/licenses/by/4.0/>)

How to cite this article:

Shafik, C. Gamil, Elshahat, M. Rabah, Mahmoud, A. Abdelghani and Mostafa, A. Ezzeldeen Ahmed (2026). Extending The Life Cycle of Self-Healed Asphalt Pavements with Recycled Additives. Journal of Rehabilitation in Civil Engineering, 14(2), 2287. <https://doi.org/10.22075/jrce.2025.2287>

1. Introduction

One of the most popular surface materials used for paving is asphalt mixture because it offers outstanding mechanical performance, cost-effectiveness, short construction period, and abrasion resistance [1–3]. It is made up of a combination of coarse and fine aggregates, asphalt binder, and air voids [4]. These materials must withstand all traffic loads for a long time in good conditions and under numerous different environmental conditions [5].

Asphalt mixes are separated into four types based on mixing temperature: hot mix asphalt, warm mix asphalt, half warm mix asphalt, and cold-mix asphalt. Among all these four mixtures, hot mix asphalt (HMA) is the most used in road construction due to its several advantages, such as high resilience, durability, waterproofing, and the protection of other road layers by decreasing the stresses of traffic due to its high stiffness [6]. It should be noted that additives, including organic and chemical additives, are used during the preparation of warm mix asphalt (WMA) and half-warm mix asphalt (HWMA) [7–9].

Additives have a great effect on improving the performance of asphalt mixtures. According to earlier studies, polymer-modified asphalt (PMA) cement can be used to produce the needed quality improvements in asphalt cement [10,11]. Crumb rubber or plastic waste added to asphalt mixtures plays a significant role in promoting cracking properties, which results in a greater number of cycles completed before cracking appears [12].

Nano-materials like Nano silica and Nano carbon are utilized to enhance the mechanical properties and moisture sensitivity of asphalt pavement, as well as the quality and behavior of bitumen under various conditions [13–15]. By incorporating nanomaterials, asphalt mixtures not only enhance strength, toughness, and resistance to common issues such as cracking, rutting, fatigue, and aging but also improve the durability of pavements. This advancement reduces the need for frequent repairs and reconstruction, conserving resources and lowering emissions in the process. Also, the industry can achieve greener production processes, lower energy consumption, and promote the use of sustainable, recycled materials [16].

The use of steel slag in asphalt mixture improves skid resistance in dry and wet conditions and fatigue failure resistance [17,18]. Pavements become less durable over time due to numerous factors, including the composition of the aggregate, bitumen rheological properties, the type of mixture, and the effects of the environment and traffic after construction. Cracks are one of the main types of pavement deterioration. Pavement cracks can be caused by the repetition of traffic loads, moisture, and rapid temperature changes.

These cracks affect driving safety and comfort, reducing pavement service life. In addition, water can penetrate the road surface through the cracks to the underlying layers, which decreases the pavement layer's stability and causes water damage that will lead to further deterioration, such as potholes and pavement structure failure, which requires more frequent maintenance or rehabilitation [19,20]. The other problem in asphalt mixtures that leads to pavement failure, such as surface ravelling and cracking, is the bitumen aging that occurs over time.

Bitumen aging refers to the process by which the stiffness or viscosity of bitumen increases over time. As a visco-elastic material, the behavior of bitumen is significantly influenced by temperature and the rate at which a load is applied. Bitumen can be divided into two main components: asphaltenes and maltenes. Asphaltenes are the unsolved parts of bitumen in n-heptane, while maltenes are the solved parts.

The aging mechanism of bitumen is the transformation of maltenes into asphaltenes, which have a higher molecular weight. As the proportion of asphaltenes in the bitumen content increases, its hardness rises, resulting in lower penetration and higher viscosity [21].

When the pavement is subjected to environmental factors as heat, oxygen, and ultraviolet light (UV), the bitumen will be susceptible to aging, and the pavement performance will deteriorate, causing many asphalt pavement distresses as spalling, looseness, and cracks [22]. Bitumen aging and crack formation are the most significant problems related to the reduction in durability [23].

To achieve long-lasting pavements, it is necessary to control the evolution of cracks and repair them before they become deeper and deteriorate the lower layers, which are less accessible and cost more to repair [24]. Recently, alternative maintenance methods have been investigated due to both economic and environmental reasons. One of these methods is based on the healing mechanism of bituminous materials [21]. Self-healing is known as the capability of a material to automatically heal (repair) the cracking that happens during its service life [25]. This means that bitumen can recover damage in hot weather and/or when there have been a lot of rest periods, extending the service life of the pavements [26].

The self-healing procedure in asphalt mixes may be influenced by several internal and external factors. The most significant internal factors that impact self-healing in bituminous pavements are the type of bitumen used and its chemical properties, bitumen content and viscosity, gravity, aggregate gradation and structure, surface tension, and characteristics of the mixture's volume. The external factors are categorized as healing temperature, crack level, rest period, aging level, and applied stresses [25]. Rapid changes in temperature will drive bitumen to fill the cracks fast, so lower viscosity bitumen will heal more quickly than higher viscosity bitumen [27]. Additionally, asphalt mixtures with higher bitumen-to-aggregate ratios might have better self-healing capabilities [28,29].

Asphalt self-healing has a significant impact on the asphalt road's durability, but at ambient temperatures, it only occurs over a few hours or days, making it exceedingly ineffective and uncontrollable. For this reason, there are mainly two technologies that have been developed to increase the self-healing effectiveness of asphalt mixes: (1) using heating sources, electromagnetic or induction heating [30], and (2) adding encapsulated bitumen solvents within the mixture [31]. These two techniques work by momentarily changing bitumen viscosity in the mix of fractured asphalt, which upsets the state of equilibrium that maintains the bitumen stable and forces it to flow through the cracks [28,32].

The first self-healing technique uses electromagnetic heating, in which conductive particles such as SWF, cast iron particles, cast steel particles, magnetite particles, Steel Shavings, and steel slag are added to the asphalt mixture and heated using an induction or microwave field. This causes the bitumen to melt and flow into the cracks. However, the bitumen may age as a result of the high temperatures. This technique requires an external source to heat the conductive particles [33,34].

In the second self-healing technique, the asphalt is mixed with encapsulating bitumen solvents, such as vegetable oils, palm oil, or waste oils (i.e., vegetable oils and mineral oils). When cracks appear in the pavement, the compressed solvents released from the capsules soften the mixture locally. This encourages the compaction of aggregates, which seals cracks. This self-healing mechanism may encourage rutting and decrease the rigidity of the asphalt. The capsules must be impermeable to the solvents and withstand mixing and compaction in asphalt [21,35].

There are other methods of self-healing technology by the use of nano-materials or polymers with asphalt healing properties. These techniques aim to enhance the healing capabilities of asphalt and optimize the composition design of asphalt mixtures, making it possible to achieve multiple active healing effects within the micro-cracks of the pavement system under specific temperature conditions [36,37].

Numerous investigations have been conducted on the self-healing properties of asphalt pavement, and the following results have been obtained:

Rest intervals included in the initial stages of the fatigue test extend the fatigue life and significantly impact the asphalt binders' ability to recover and increase the total number of loading cycles before failure

occurs [25]. The ability of asphalt mixtures to heal themselves improved with an increase in healing temperature and duration, while decreasing with an increase in notch length [38]. The creation of cracks affects how well an asphalt mixture heals itself. With the use of microwave and induction heating [39], it is possible to repair asphalt mixtures by heating both the Fibers and the aggregates; however, the high percentage of fibers results in a negative effect on the mechanical properties [40,41].

Fiber additives can enhance induction heating by establishing conductive paths that support the conduction energy conversion mechanism [42]. Steel slag's chemical composition and mineral constituents can be used to explain why it can absorb microwave energy [43,44]. It was also found that by applying an alternating magnetic field (AMF), iron-based particles could be incorporated into bituminous materials to act as local heat sources for efficient crack healing. Iron-based particles with diameters less than 1 mm prevent the temperature from rising in the sample, preventing the bituminous material from unintentionally overheating [33].

This paper aims to address several key issues related to road infrastructure. First, the prevalence of road deterioration and cracks significantly decreases the effectiveness and life cycle of the roads, leading to increased accident rates and necessitating extensive repair and rehabilitation efforts. Secondly, the escalating costs of road repairs have become a considerable financial burden for the government, requiring substantial investments to restore the roads to their previous level of performance. Additionally, the depletion of natural resources and the accumulation of waste materials, particularly steel construction by-products, pose disposal challenges that need to be mitigated.

On the other hand, Self-healing asphalt could eventually reduce greenhouse gas emissions and lower maintenance costs. Additionally, it is now common practice to use recycled materials like Fibers and steel Slag in asphalt mixtures to (1) increase thermal conductivity and homogenize heating in the mixtures; (2) produce asphalt road pavements that are environmentally sustainable, and (3) conserve natural resources. So, the main objective of this paper is to produce a sustainable asphalt mixture using SWF or EAFS.

Previous studies on sustainable asphalt mixtures have primarily focused on the effects of high percentages of steel wool fiber (SWF) and electric arc furnace slag (EAFS) as partial replacements for traditional materials. However, these studies often overlook the optimization of SWF content and length, specifically how lower percentages and varied lengths can influence the overall mechanical properties and performance of hot mix asphalt (HMA) while minimizing air void content.

Additionally, while EAFS has been investigated as an aggregate replacement, existing research typically limits its use to specific sieve sizes rather than exploring its potential as a broader coarse aggregate replacement. This gap in the literature indicates that there is a lack of comprehensive understanding of how these materials can be integrated in a way that maximizes the benefits of both SWF and EAFS.

This paper investigates the effects of using lower percentages and varying lengths of SWF in combination with EAFS as a coarse aggregate replacement. This approach aims to enhance the mechanical properties, reduce air voids, and ultimately contribute to the development of a more sustainable asphalt mixture. By addressing these overlooked areas, the research aims to provide valuable insights for future applications in road infrastructure, promoting both environmental sustainability and improved performance.

The objectives of this study are to:

1. Develop an environmentally sustainable asphalt mixture incorporating SWF and/or EAFS.
2. Evaluate the impact of these additives on maintenance costs and pavement life cycle.
3. Assess resource efficiency by reducing reliance on natural aggregates and minimizing industrial waste.
4. Simulate pavement performance using KENPAVE software.
5. Analyze the cost-effectiveness of using SWF and EAFS in asphalt mixtures.

2. Methods

This paper consists of seven Stages as illustrated in Fig. 1.

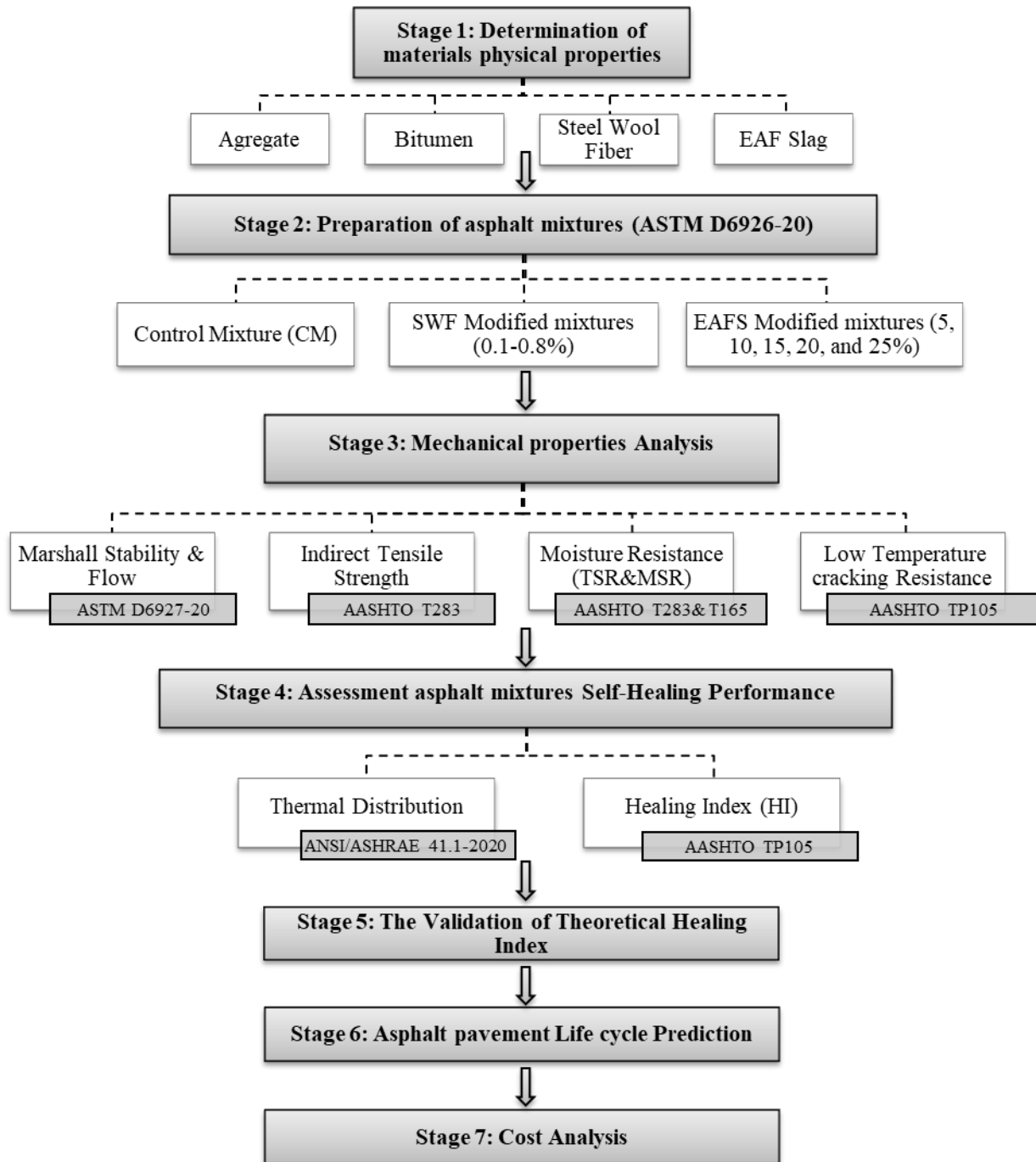


Fig. 1. Experimental Program Flowchart.

2.1. Raw materials and physical properties

The asphalt mixture was prepared (in accordance with ASTM D6926-20) using coarse aggregate, fine aggregate, filler, and bitumen with a penetration of 60/70, as it is the most commonly used in the region. The raw materials used in this study are from El Meligy Company for Integrated Contracting Works. To accelerate the self-healing property of the asphalt mixture, Steel Wool Fibers (SWF) and Electric Arc Furnace Slag (EAFS) additives were added to control mixtures.

SWF is a very fine fiber with diameters of 130 μ m and two different lengths from 1 to 4 mm and 4 to 8mm, as shown in Fig. 2a and Fig. 2b, respectively, and with a density of 7.180 g/cm³. The contents of SWF used in this study range from 0.1% to 0.8% of asphalt concrete weight. These percentages were determined based on previous studies, which indicate that higher SWF contents (exceeding 1.5% of asphalt concrete weight) adversely affect the mechanical properties of the mixture by increasing air voids [39–41]. Therefore, the lower percentages chosen (0.1 to 0.8%) aim to evaluate the effects of SWF on the self-healing properties and mechanical performance of HMA without reaching levels that could lead to negative outcomes.

The EAFS was provided by EZZ Steel Company. In this study, the EAFS was used with sizes ranging from 1.18 to 19mm (shown in Fig. 2c) as a replacement for natural coarse aggregate with percentages ranging from 5% to 25% with an increment of 5% from the total weight of the asphalt mixture. Those percentages correspond to the percentages used in previous studies [44,48]. The physical properties of bitumen and aggregate are shown in Tables 1 and 2, respectively. Table 3 illustrates the chemical analysis of Electric Arc Furnace Slag, as shown in our studies [49].

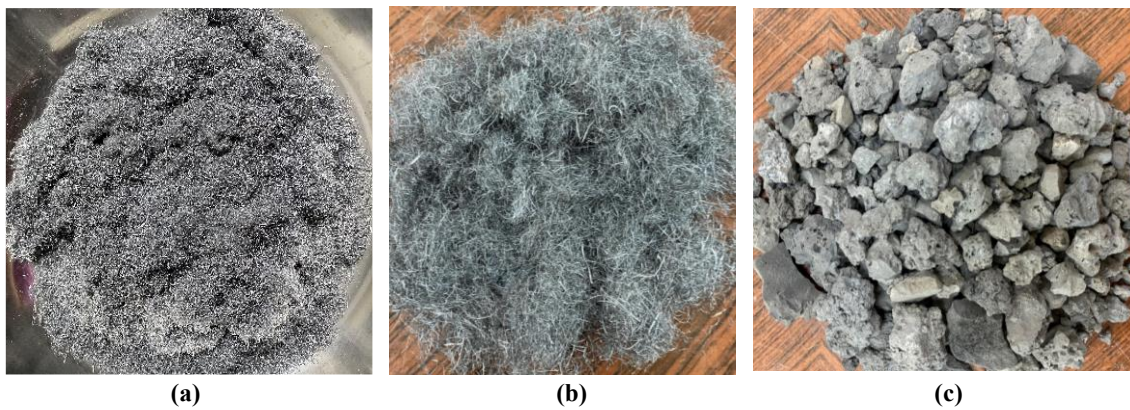


Fig. 2. Self-Healing Materials: (a) Short SWF, (b) Long SWF, and (c) EAFS.

Table 1. Bitumen physical properties [49].

Test	Specification	Results	Limits
Penetration (25°C, 100g, 0.1S) 0.01mm	ASTM D5-06	67	60 – 70
Kinematic Viscosity (135°C, CST)	AASHTO T 201	369	+ 320
Softening point (°C)	ASTM D36	53	45- 55

Table 2. Aggregate Physical Properties [49].

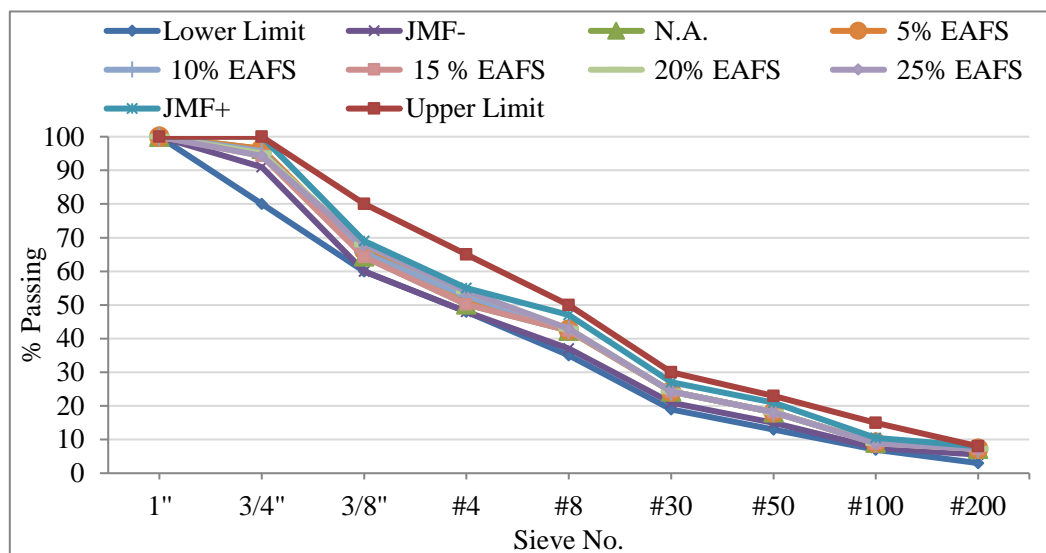
Test	Specs.	N.A. (25-20) mm	N.A. (19-16) mm	EAFS (2.36-13) mm	EAFS (13-19) mm	Limits
Abrasion value (%) after 500 laps after washing	(ASTM C131)	19.16%	20.16%	20.20%	16.60%	not exceed 40%
Abrasion value (%) after 100 laps after washing		4.20%	5.06%	4.40%	4.00%	not exceed 10%
Bulk Density	(ASTM C127)	2.566	2.650	3.194	3.367	-
Bulk SSD S. G		2.612	2.684	3.311	3.44	-
Apparent S. G		2.689	2.743	3.616	3.632	-
Absorption (%)		1.77	1.27	3.656	2.165	not exceed 5%

Table 3. Chemical Analysis Of Electric Arc Furnace Slag [49].

MgO	SiO ₂	Al ₂ O ₃	Fe ₂ O ₃	CaO	SO ₃	MnO	Na ₂ O	Cr ₂ O ₃	V ₂ O ₅	P ₂ O ₅	TiO ₂	K ₂ O
%	%	%	%	%	%	%	%	%	%	%	%	%
5.82	13.96	6.59	36.44	33.52	0.10	1.98	0.02	0.40	0.14	0.49	0.54	0.01

2.2. Asphalt mixtures

To obtain the research objective, three Dense Asphalt mixtures were developed: control mixtures (CM), SWF-modified mixtures, and EAFS-modified mixtures. Available aggregate sizes are combined in different percentages to get the proper dense asphalt mixture gradation using the mathematical trial method; the selected gradation was 4C. The gradation of the control asphalt mixture and EAFS-modified mixture was presented in Fig. 3 with lower and upper limits and Job Mix Formula (JMF) limits. According to Hot Mix Design, the optimum bitumen content (OBC) that meets maximum bulk density, maximum stability, and air voids (3-5%) was 5%. This percentage will be used in all mixtures to compare the effect of adding self-healing additives to the control mixture. Table 4 summarises the Modified Asphalt Mixtures formulation.

**Fig. 3.** Natural Aggregate and EAFS Gradation.**Table 4.** The Modified Asphalt Mixtures Formulation.

Mixtures	Control Mixtures	EAFS-Modified Asphalt Mixture					SWF-Modified Asphalt Mixture				20% EAFS+ 0.2% SWF Modified Asphalt Mixtures*
N.A.%	100	95	90	85	80	75	100	100	100	100	80
EAFS%	-	5	10	15	20	25	-	-	-	-	20
SWF%	-	-	-	-	-	-	0.2	0.4	0.6	0.8	0.2

* This mixture is used in asphalt pavement life cycle prediction and cost analysis

3. Results and discussions

3.1. Marshall stability and flow

The Marshall Stability and Flow Test was performed in accordance with ASTM D6927-20. The Marshall Method, which is primarily empirical, is helpful in comparing mixes under certain conditions. This technique involves using the Marshall apparatus (shown in Fig. 4a) to load cylindrical bituminous paving mixture specimens on the lateral surface and measuring the specimens' resistance to plastic flow. Marshall

Stability describes the highest load value that a sample can support during testing at 60 °C, and Marshall Flow describes the deformation that a sample goes through during loading up to the highest load. The ability of an asphalt mixture to resist shoving and rutting under heavy traffic load is improved when the Marshall Stability value increases. The Marshall Quotient, also known as stiffness, is the stability-to-flow ratio. In this paper, the Marshall stability and flow test was used to determine the OBC for mixtures and to evaluate how well the modified asphalt mixture performed.

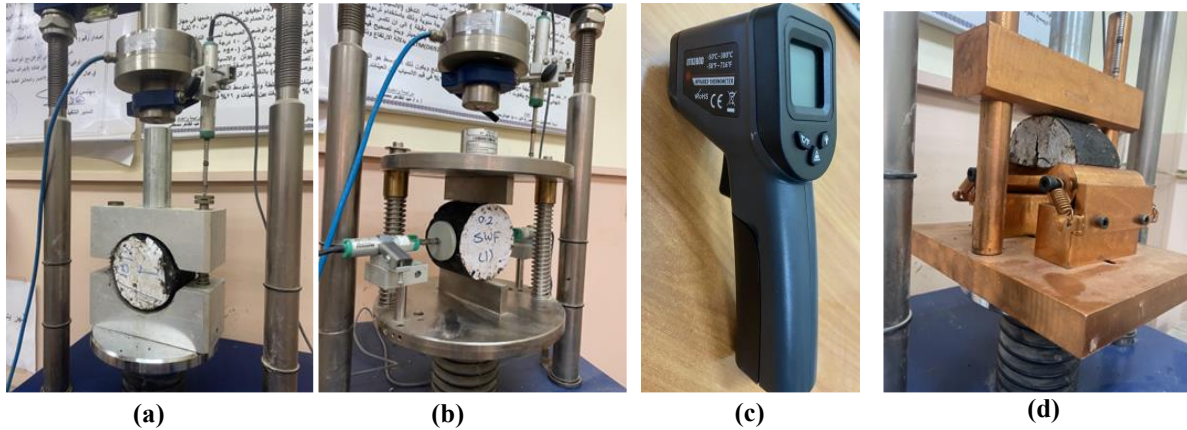


Fig. 4. Apparatuses used in this paper: (a) Marshall Apparatus, (b) ITS Apparatus, (c) infrared thermometer and (d) TPB Apparatus.

3.1.1. Marshall test result for eafs-modified asphalt mixture

The Marshall test results of asphalt paving mixtures containing EAFS are illustrated in Table 5.

Table 5. Marshall Test Results for Asphalt Paving Mixes Containing EAFS.

% of EAFS	Stability (kg)	Flow (mm)	Marshall Quotient MQ (Kg/mm)	AV %	VMA %	VFB %	Bulk density (t/m ³)
0%	1356.02	2.623	516.973	4.200	15.600	65.385	2.330
5%	1376.31	2.614	526.515	4.782	14.554	66.019	2.337
10%	1449.00	2.588	559.892	4.438	13.826	67.902	2.364
15%	1530.00	2.509	609.805	3.971	13.502	70.704	2.400
20%	1586.98	2.399	661.517	3.557	13.318	79.121	2.434
25%	1560.27	2.543	613.555	3.018	12.847	83.442	2.476

As illustrated in Table 5, it has been demonstrated that the Marshall Quotient (MQ) increases significantly when Electric Arc Furnace Slag (EAFS) is used to replace natural aggregates, reaching its maximum value at 20% EAFS before decreasing. This increase in MQ is attributed to the higher Marshall stability and the lower Marshall Flow. The incorporation of EAFS into hot mix asphalt enhances its compatibility with bitumen and resistance to stripping while also improving stability and preventing rutting and fatigue cracking due to its shape and rough surface texture. This is compatible with previous studies [44, 45]. Specimens with 20% EAFS have the highest values of Marshall stability and the lowest value of Marshall flow compared to other EAFS percentages and control samples, which indicates that modified asphalt mixtures with EAFS up to 20% have high load-withstanding strength and high rutting resistance.

When EAFS is added to the asphalt mixture, AV and VMA decrease, while VFB increases, as illustrated in Table 5. The shape particle, gradation, and maximum nominal size of the used EAFS significantly influence the determination of these values. In terms of self-healing, a positive correlation between EAFS and temperature rise should support the Healing Index (HI). In addition, VFB also describes the amount of free asphalt in the mixture, which is necessary for self-healing. More free asphalt can flow and fill in cracks after being exposed to heating sources, which is generally a result of higher VFB. Therefore, higher EAFS led to greater healing performance. Higher cohesion and adhesion within the asphalt mixture

would improve the low-temperature cracking resistance because of the high free bitumen content. For VMA%, specimens with 25% EAFS have a VMA% lower than the limits (13.2% according to MORTH specifications). Therefore, this percentage will be ignored in the self-healing performance index section. As illustrated in Table 5, the bulk density demonstrated a steady rise as EAFS increased. Compared to the Reference mixture, mixes containing EAFS exhibited much higher bulk densities. This is brought on by the fact that natural aggregates have lower specific gravities than EAFS, increasing the bulk density of the mixtures.

3.1.2. Marshall test result for swf-modified asphalt mixture

Table 6. Marshall Stability and Flow for Asphalt Paving Mixes Containing Different SWF Lengths.

% of SWF	SWF (1-4mm) Length			SWF (4-8mm) Length		
	Stability (Kg)	Flow (mm)	Marshall Quotient MQ (Kg/mm)	Stability (Kg)	Flow (mm)	Marshall Quotient MQ (Kg/mm)
0.0%	1356.018	2.623	516.972	1412.341	2.563	551.050
0.1%	1380.492	3.115	443.176	1403.310	2.475	566.994
0.2%	1464.958	2.854	513.300	1386.134	2.432	569.956
0.3%	1593.816	2.708	588.558	1356.215	2.426	559.033
0.4%	1665.094	2.620	635.532	1318.289	2.451	537.858

It's demonstrated that while the increase in short SWF content has a positive effect on the Stability of asphalt mixture, an increase in long SWF content has the opposite effect [47]. As illustrated in Table 6, Marshall Stability of the asphalt mixture with short SWF increases as the SWF percentages increase, while the stability of asphalt mixture with Long SWF decreases as the SWF percentages increase, but all values are higher than limits (according to MORTH specifications, the stability for heavy roads must be greater than 920 Kg). Stability decreased for Long SWF mixtures due to the clustering caused by fibers within the mixture, leading to a potential loss of interaction between aggregate particles. So, short SWF has higher load-withstanding strength than long SWF. The Marshall flow Results for short SWF decrease as the SWF percentages increase, while the Marshall flow result of asphalt mix with Long SWF decreases, then increases as the SWF percentages increase. Samples with high Marshall flow values have lower rutting resistance than samples with low Marshall flow values; therefore, in terms of flow, mixtures with long SWF have higher rutting resistance than short SWF mixtures.

Also, Table 6 illustrates that the Marshall Quotient (MQ) increases with the increase of long SWF content until it reaches the highest MQ at 0.2% and then decreases. For short SWF content, MQ increases with the increase in SWF content.

Table 7. Volumetric Properties and unit weight results for Asphalt Paving Mixes Containing different SWF Lengths.

% of SWF	SWF (1-4mm) Length				SWF (4-8mm) Length			
	AV %	VMA %	VFB %	Bulk density (t/m ³)	AV %	VMA %	VFB %	Bulk density (t/m ³)
0.0%	4.5	15.258	64.597	2.295	4.2	15.6	67.235	2.330
0.1%	4.997	14.816	62.633	2.298	4.280	15.211	68.695	2.330
0.2%	4.982	14.480	63.146	2.303	4.359	14.845	67.943	2.327
0.3%	4.929	14.112	63.849	2.313	4.445	14.515	66.790	2.324
0.4%	4.887	13.765	65.218	2.322	4.538	14.245	65.215	2.322

Table 7 illustrates the volumetric properties of the asphalt mixtures for two different lengths of SWF. For long SWF, when SWF Content increases, AV% increases gradually; meanwhile, VFB decreases. Theoretically, SWF is expected to have a positive correlation with temperature increment, improving the healing rate. In addition, voids filled with bitumen (volume of free bitumen) in the mixture have an important role in self-healing. As previously indicated, higher VFB% results in more bitumen that is free

to flow and fill cracks after sample exposure to a heating source. Consequently, even though heating efficiency increased with higher SWF content, its detrimental effects on free bitumen should not be disregarded. This explains why raising SWF does not always increase the Healing Index (HI). On the other hand, Short SWF reduces AV% and increases VFB. Although the heating efficiency increased and the void filled with bitumen increased with the rise of short SWF, Short SWF does not lead to an increase in HI. This could be because the length of the SWF is too short to have the ability to heat the samples. VMA% increases with an increase in SWF content for Long SWF, while it decreases for Short SWF. For Long steel wool fiber, the bulk density showed a constant decrease as it increased in SWF content, while the Short SWF had the opposite effect, bulk density increased with the increase of SWF content, as illustrated in Table 7.

After investigating the effect of different SWF lengths on the mechanical properties, we made trial samples to investigate their effect on healing properties, as it is the goal of our paper. Our findings revealed that short SWF does not lead to an increase in HI. The highest HI value was observed for 0.2% SWF heated by microwave, which was 45.56%, and 35.09% for induction heating. This could be because the length of the SWF is too short to generate sufficient heat to enhance the samples' healing properties. Conversely, long steel wool fibers demonstrated a significant impact on self-healing performance, with an HI of up to 90%. Therefore, we analyzed long SWF with a percentage range of 0.2% to 0.8%, with an increment of 0.2%. This analysis allowed us to obtain a clearer understanding of the impact of SWF on the healing properties.

3.2. Indirect tensile strength (ITS)

The failure of the specimen in the ITS test is attributed to a lack of bitumen and aggregate adhesion, which is a sign of the mixture's performance and durability. The ITS is carried out in accordance with AASHTO T283 (Testing Machine is shown in Fig. 4 b) and is calculated as Eq. (1):

$$ITS = (2 * P) / (\pi * t * D) \quad (1)$$

Where: ITS: sample Indirect Tensile Strength (MPa), P: Maximum Load (N), t: specimen thickness (mm), D: specimen Diameter (mm).

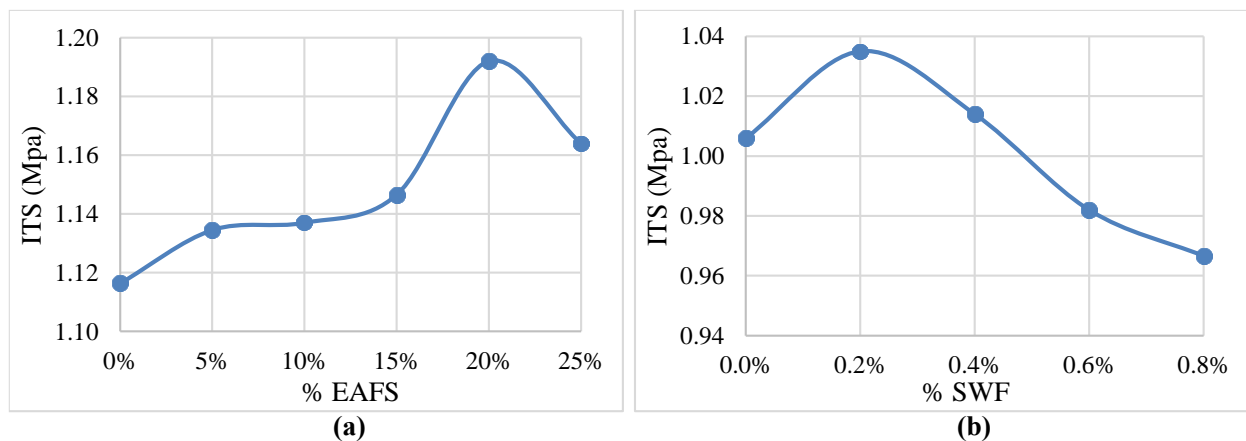


Fig. 5. Indirect Tensile Strength (a) EAFS, and (b) SWF.

Using five different percentages of EAFS and four percentages of SWF, the ITS test was conducted to determine the specimens' shear resistance. It was found that all EAFS-modified asphalt mixtures have shear resistance higher than control mixtures, while in SWF-modified mixtures, only 0.2% and 0.4% SWF have shear resistance higher than control mixtures. The best shear resistance was at 20% EAFS and 0.2% SWF, with values exceeding the control mixture by 6.78% and 4.44%, respectively, as depicted in Fig. 5a and Fig. 5 b.

3.3. Moisture resistance

The surface layer of pavement needs to be durable enough to withstand the impacts of weather, water, temperature, and vehicle friction. This durability is essential to ensure that the pavement is protected from damage. So, the Tensile strength ratio test (AASHTO T 283) and the Marshall immersion test (AASHTO T165) were conducted to evaluate the moisture resistance (water stability) of the mixture. The Tensile Strength Ratio (TSR) is calculated according to Eq. (2):

$$\text{TSR} = \text{ITS}_2 / \text{ITS}_1 \quad (2)$$

where: ITS_1 : average tensile strength of the dry subset (unconditioned case), (kPa), ITS_2 : average tensile strength of the conditioned subset, (kPa).

During the Marshall immersion process, we will compare the stability of two cases: one soaked for 24 hours and the other soaked for 30 minutes. This will allow us to calculate the Marshall Stability Ratio (MSR) for each case. The MSR refers to the residual Marshall stability after soaking in water at 60°C for 24 hours. By comparing the Marshall stability of the two cases at 60°C for 24 hours and at 60°C for 30 minutes, we can determine which mixture is more durable. The higher the MSR value, the greater the potential for the mixture's durability. MSR was calculated by Eq. (3):

$$\text{MSR} = \text{MS}_2 / \text{MS}_1 \quad (3)$$

where, MSR: the average residual stability of the specimen in moisture; MS_1 : the average stability of the specimen in moisture at 60°C for 30 min; MS_2 : the stability of the specimen in moisture at 60 °C for 24 hours.

3.3.1. Tensile strength ratio (TSR)

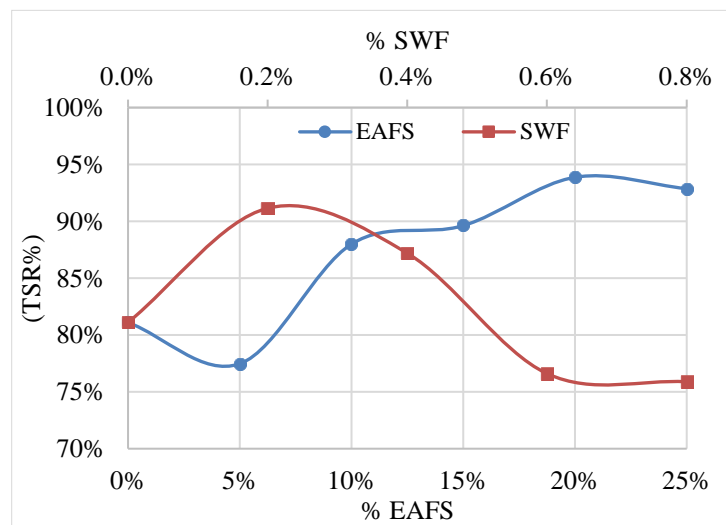


Fig. 6. Tensile Strength Ratio (TSR).

It can be shown from Fig. 6 that the TSR values increase with increasing EAFS percentages until they reach 20% EAFS, and then they decrease. Additionally, the TSR decreases with the increase of SWF. The maximum TSR was observed at 20% EAFS and 0.2% SWF. All modified asphalt mixtures have TSR% values higher than the control mixtures, except for 0.6% SWF and 0.8% SWF.

3.3.2. Marshall stability ratio (MSR)

The trend of MSR is similar to TSR. For EAFS mixtures, the MSR increases to 20% EAFS, then decreases, and for SWF mixtures, the MSR reduces with the rise in SWF content as shown in Fig. 7. The highest MSR was recorded for 20% EAFS and 0.2% SWF, with 94.52% and 93.73%, respectively. All modified mixtures were found to have a higher MSR than the CM.

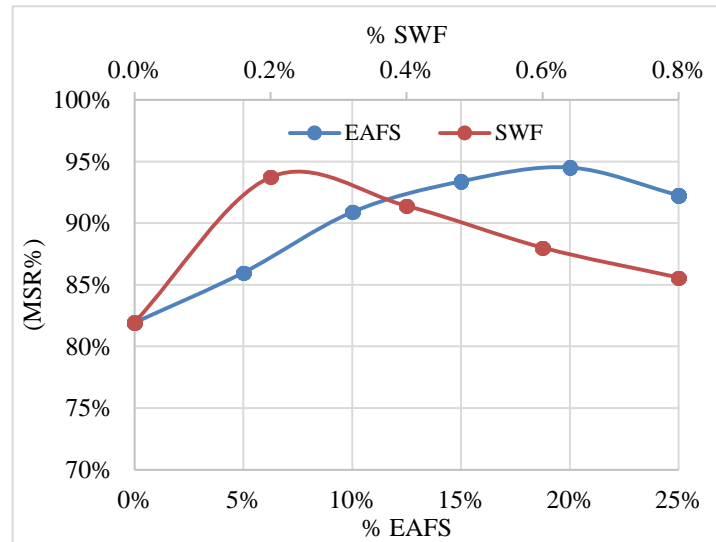


Fig. 7. Marshall Stability Ratio (MSR).

3.4. Low temperature cracking resistance

This paper studies two primary fracture parameters obtained from the TPB test (Testing Machine is shown in Fig. 4d): fracture toughness and fracture energy. These parameters determine the resistance of asphalt concrete to crack initiation and propagation within asphalt pavements under static loads. The resistance of materials to crack growth is measured using the fracture energy G_f . However, the ability of a material to resist the initiation of a crack is measured by fracture toughness K_{Ic} . The calculation of the fracture toughness and energy of TPB specimens are explained by Eqs. (4, 5, 6) according to [52]:

$$G_f = W_f / A_{lig} \quad (4)$$

$$K_{Ic} = \sigma_{max} * \sqrt{\pi a} * Y_1 \quad (5)$$

$$\sigma_{max} = P_{max} / (D * B) \quad (6)$$

Where: G_f = fracture energy (J/m^2); W_f = fracture energy (J); A_{lig} = ligament area (m^2); K_{Ic} is the sample fracture toughness; σ_{max} is the ultimate horizontal stress at failure; P_{max} is the ultimate force; D is the sample diameter; B is the specimen thickness; and Y_1 is the dimensionless stress intensity factor.

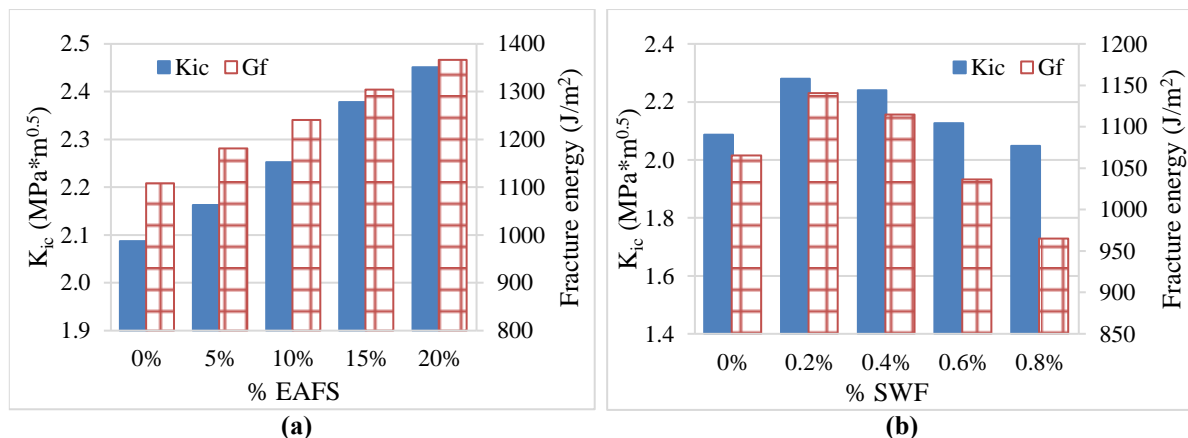


Fig. 7. Low Temperature Cracking Resistance (a) EAFS, and (b) SWF.

Fig. 8a illustrates the relationship between EAFS with K_{Ic} and G_f . As the EAFS percentage increases, the fracture toughness also increases. The highest fracture toughness value of $2.45 MPa \cdot m^{0.5}$ was achieved at 20% EAFS content, which is 17% greater than the control mix.

A mixture with high fracture energy values indicates strong cracking resistance. As depicted in the graph, fracture energy also increases with an increase in EAFS percentage, resulting in improved low-temperature cracking resistance. The specimen that demonstrated the highest fracture parameters was observed at 20% EAFS content. On the other hand, the lowest fracture parameters were recorded at 5% EAFS, which is still higher than the control. The low-temperature cracking resistance is positively correlated with higher fracture toughness and fracture energy values at a temperature of -15°C .

The results show that for the asphalt mixture modified with SWF, the fracture toughness decreases as the SWF content increases, as shown in Fig. 8 b. However, all values except for 0.8% SWF content exceeded the control mixture value. The highest fracture toughness value of $2.28 \text{ MPa}\cdot\text{m}^{0.5}$, which was 9% higher than the control sample, was achieved with 0.2% SWF content. For SWF fracture energy, it was observed that the fracture energy decreases as the SWF content increases, and only 0.2% and 0.4% values exceeded the control sample, as shown in Fig.8b. The lowest fracture energy was obtained at 0.8% SWF content, indicating that too much SWF can lead to a weakening of fracture toughness. On the other hand, G_f values of 0.2% and 0.4% were greater than those of the control mixture by 7% and 4.6%, respectively.

As illustrated in Table 6, adding long SWF to the asphalt mixture causes an increase in AV% and a decrease in VFB%. Less free bitumen in a mixture with SWF would lead to less adhesion and cohesiveness within the asphalt mixture, which would reduce the asphalt mixture's resistance to low-temperature cracking. However, SWF's toughening and strengthening properties also increased the low-temperature crack resistance. As a result, the reduction in voids filled with bitumen and the effects of higher steel wool fiber on reinforcing and lower adhesion and cohesion had a combined impact on low-temperature crack resistance.

3.5. Thermal analysis

The surface temperature of HMA specimens heated by induction heating and microwaves will be measured in this experiment. Utilizing an infrared thermometer (shown in Fig. 4c), these measurements are made. The test starts at room temperature, and then the surface temperature is measured with an interval of 1 minute for induction heating and about 10 seconds for microwave heating until the samples reach a temperature of about 90°C . According to prior studies and observations, the test sample will produce excellent self-healing results at 90°C without overheating [5,39].

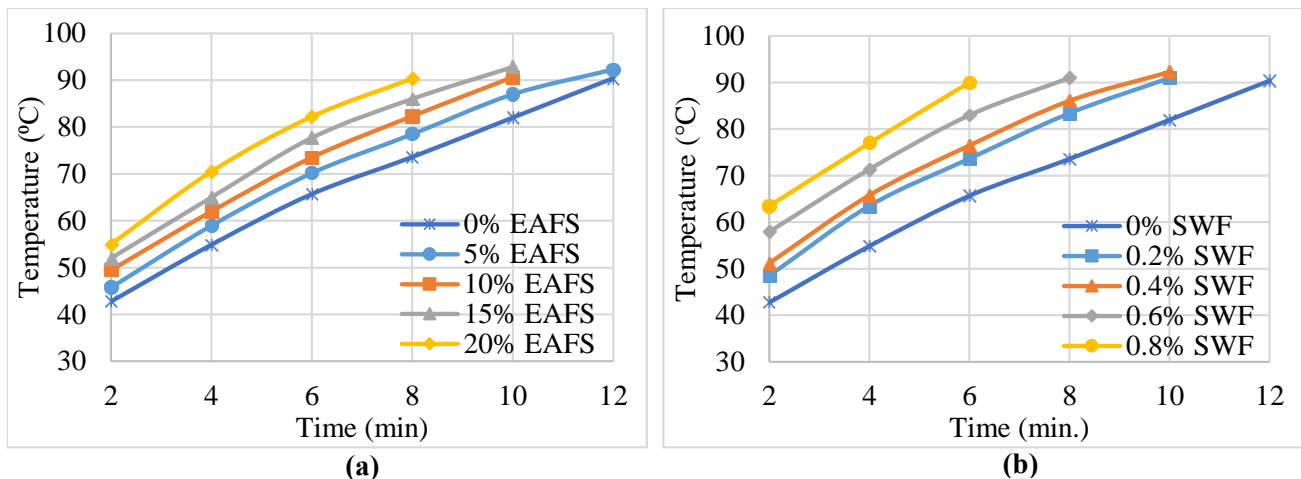


Fig. 8. Induction Heating thermal distribution (a) EAFS and (b) SWF.

The thermal distribution results demonstrate that adding EAFS to the asphalt mixture increases the surface temperature for both induction and microwave heating as shown in Fig. 9a and Fig. 10a. The reason for this is the high percentage of the O element which increases the mixture's complex permittivity and loss angle, enhancing the mixture's ability to absorb electromagnetic waves also the higher thermal

conductivity of EAFS quickly transferring heat to the surrounding aggregate. For 20 % EAFS, the time consumption decreased by 33.33% for induction heating, while the time consumption for microwave heating decreased by 50%. For SWF, adding SWF to the asphalt mixture raised the mixture's surface temperature to a certain degree. The amount of SWF present determines how quickly the temperature rises over time, as shown in Fig. 9 b and Fig. 10 b. For both induction and microwave heating, the surface temperature increased as SWF content increased, while microwave heating led to bitumen aging faster than induction heating. The mixtures with 0.8% SWF have the highest decrease in time and energy consumption, it was 67.57% for microwave heating and 50% for induction heating.

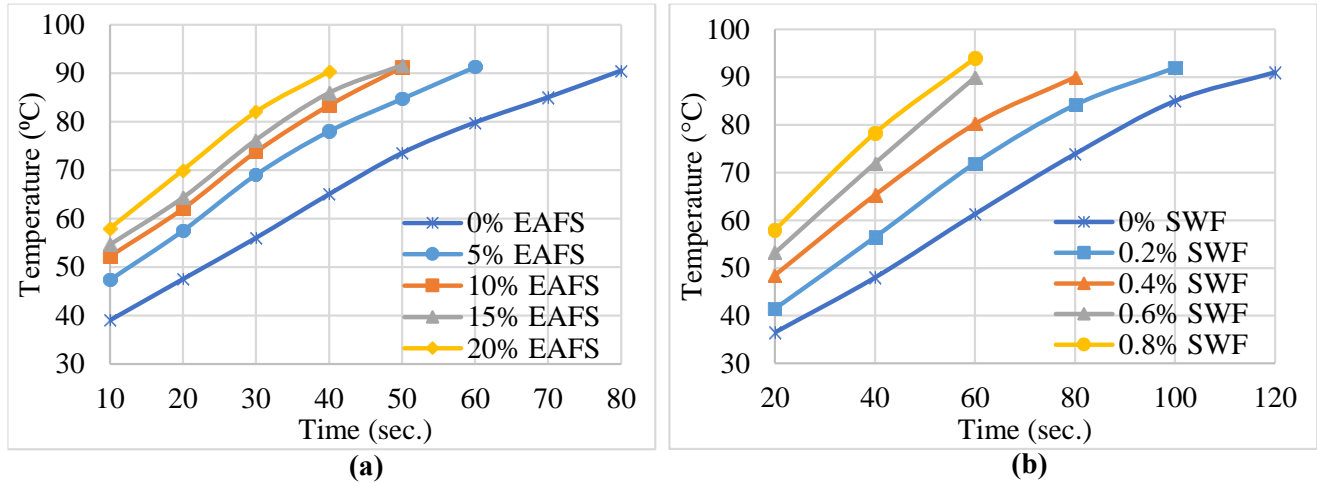


Fig. 9. Microwave Heating thermal distribution (a) EAFS and (b) SWF.

3.6. Self-healing process

To evaluate the self-healing abilities of various asphalt mixtures, the TPB test was carried out at low temperatures on asphalt concrete specimens in accordance with AASHTO TP105 standard procedures.

The crack-healing process of the samples consisted of the following steps:

- (1) Semi-circular test samples were placed onto two supporting rollers. A vertical monotonic load was positioned at the midpoint of the semi-circular arch of the sample (shown in Fig.11), and the load speed ratio was set at 0.5 mm/min. The whole testing process was conducted at a temperature range of around -18 °C. The TPB strength of the sample was defined as the maximum load it could bear, and the sample was cracked as a sign of failure.
- (2) In order to evaporate surface moisture from freezing, samples were left at room temperature for 4 h until they reached 25 °C. Half Samples were exposed to microwave heating, and the other half to induction heating (shown in Fig. 11 b).
- (3) After the heating process, the test specimens were rested at room temperature before being put into the refrigerator for 24 hours. This completed one damage-healing cycle. In order to determine the healing effectiveness of the various asphalt mixtures, a total of 4 damage-healing cycles were performed on each sample (shown in Figs. 11c and d).

The healing cycle illustrated in Fig. 11 and the healing index (HI) in this paper was established as the following ratio based on previous research [39]:

$$HI = F_i/F_0 \quad (7)$$

Where: F_0 : initial test ultimate force, and F_i : the test sample's ultimate force after the i^{th} cycle of the cracking-healing procedure.

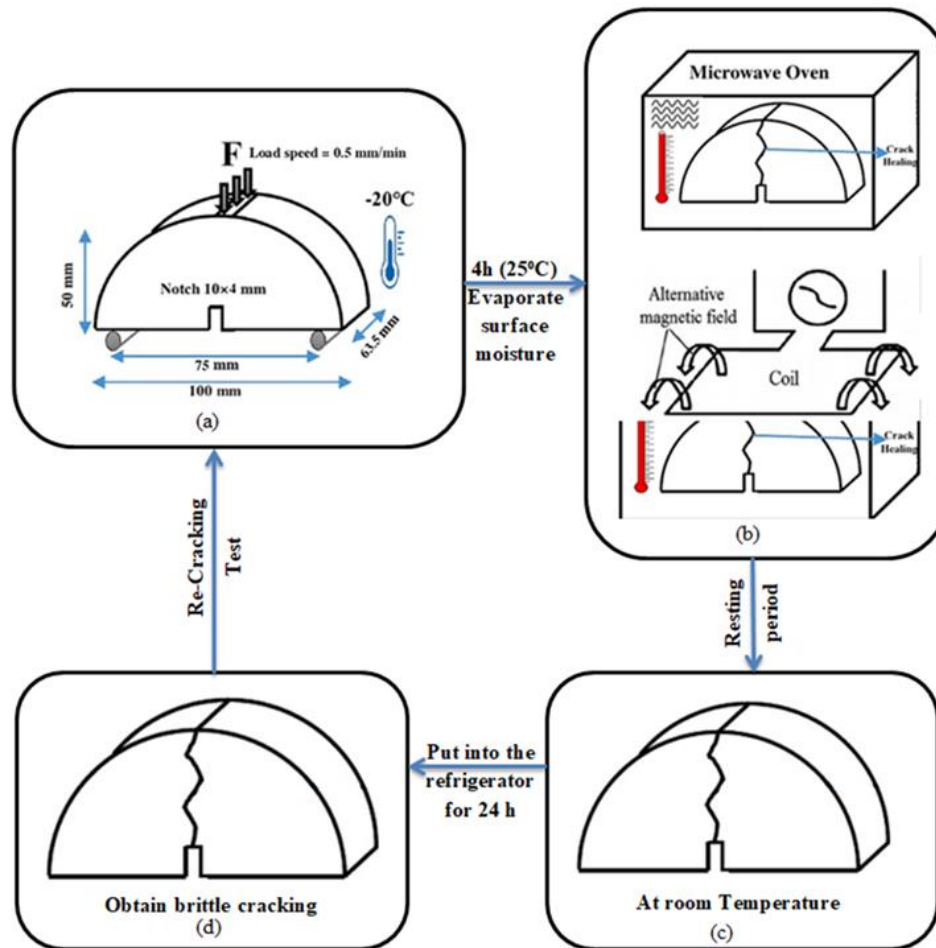


Fig. 10. A schematic diagram illustrates the cracking-healing cycle of the asphalt specimen.

3.6.1. EAFS healing index

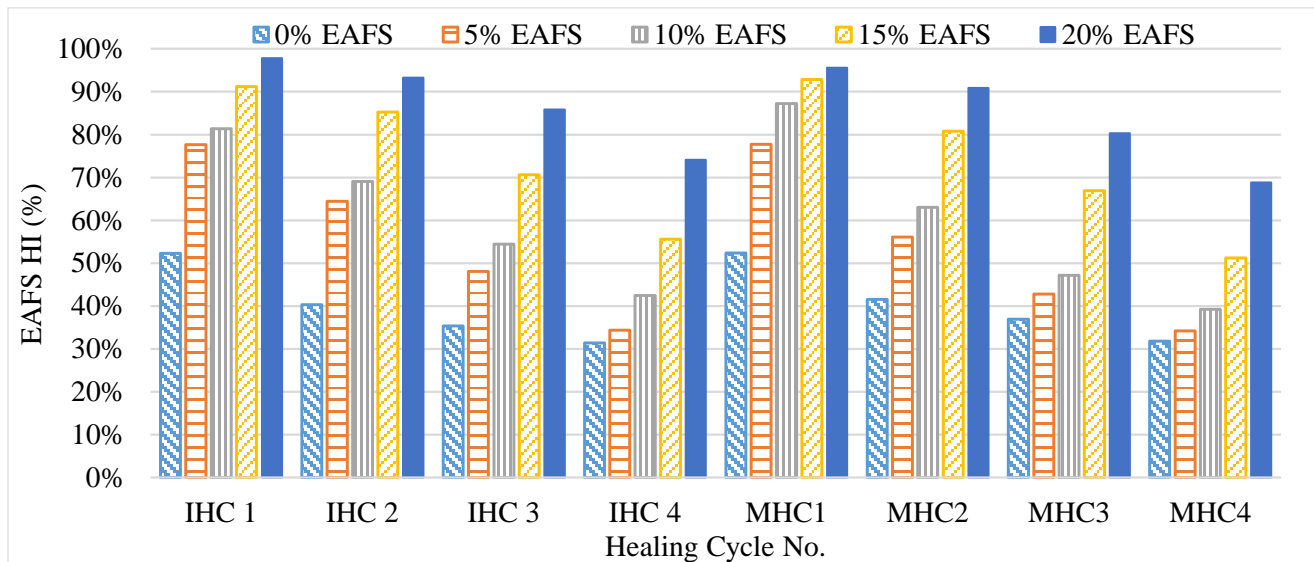


Fig. 11. EAFS Healing Index.

The Healing Index (HI) of control samples for induction heating (IH) after one loading cycle is only 52.27%. After four loading cycles, the HI drops to 31.42%. For microwave heating, the HI after one loading cycle is 52.39%, and after four loading cycles, it decreases to 31.84%. These results demonstrate the extremely poor self-healing capabilities of the control mixtures.

The induction heating (HI) of 20% EAFS is 97.8% at the first cycle and 74.08% after four cycles, which is 1.87 and 2.36 times that of the CM, respectively. After four cycles, the induction healing of 20% and 15% EAFS is above 50%. Additionally, 10% of EAFS exhibited induction healing greater than 50% after three loading cycles, compared to 5% which had a healing index greater than 50% for just two loading cycles as shown in Fig. 12. The Microwave Heating (MH) healing index of 20% EAFS is 95.5% after the first cycle and 68.81% after four cycles, which is 1.82 and 2.16 times that of the control mixture, respectively. Only the MH healing index of 15% and 20% EAFS exceeds 50% after four cycles, while 10% and 5% have a healing index higher than 50% for only two loading cycles, as shown in Fig. 12. The earlier studies show that using steel slag to replace one sieve size increases the HI [1,48]. This supports the findings in this section, even though in this paper, EAFS was used to replace all coarse aggregate sieve sizes.

3.6.2. SWF healing index

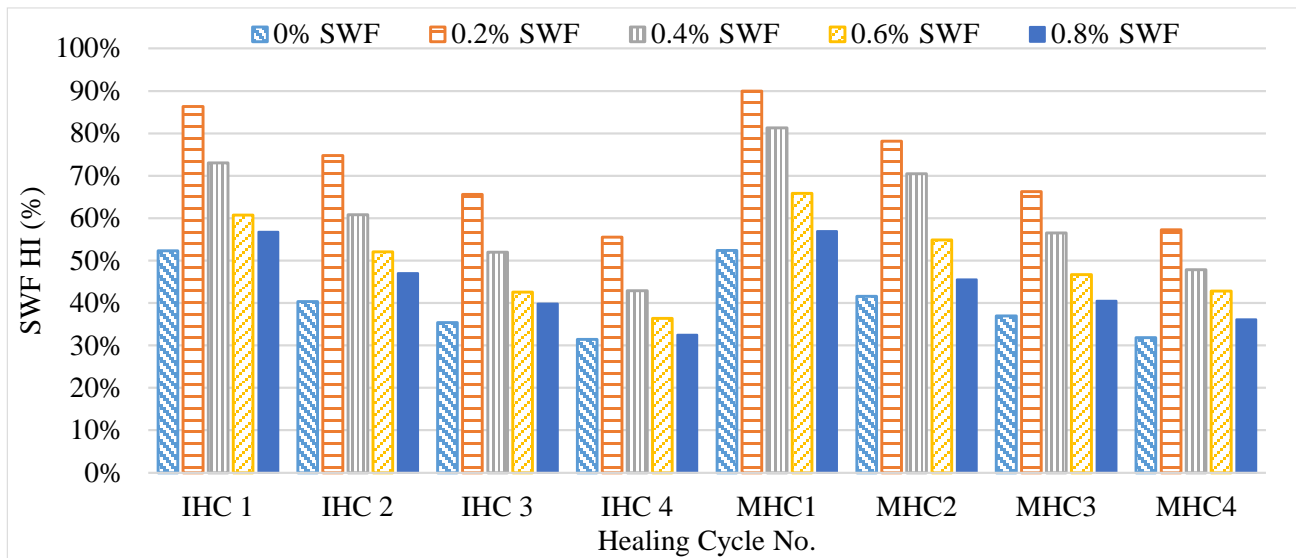


Fig. 12. SWF Healing Index.

The SWF Modified Mixture had a lower healing index than EAFS-modified mixtures. In general, the SWF-modified mix's capacity to heal decreased with increasing damage-healing cycles. The highest HI value was achieved by mixtures containing 0.2% SWF in both induction and microwave heating, but the induction heating HI was lower than the microwave heating healing index. The Induction heating HI for 0.2% SWF was 86.34% and 55.56% after the first and fourth cycles, respectively. And The Microwave heating HI for 0.2% SWF was 90% and 57.28% after the first and fourth cycles, respectively, as shown in Fig. 13. This is probably due to the best fiber distribution and the least degree of fiber aggregation found in these mixes. The least effective mixes for healing have a SWF content of 0.6% and 0.8%. It can be explained by cluster formation and inhomogeneous distribution of SWF, which causes the bitumen to age. As a result of the aged bitumen binder's high viscosity and poor flowability, the crack healing process was harder. In conclusion, the outcomes of this section support those of the earlier [47].

As mentioned before, the SWF corrosion under moisture conditioning caused a decrease in the indirect tensile strength, the tensile strength ratio (TSR), and the Marshall stability ratio (MSR) of the asphalt concrete. On the other hand, the EAFS-modified asphalt mixture has a higher moisture resistance than the SWF-modified asphalt mixture. Regarding the moisture resistance effect on the healing index, the results indicated that the heating rate of the asphalt mixture under microwave radiation is significantly higher than induction heating for the same level of moisture content. This is due to the higher sensitivity of water molecules to electromagnetic fields compared to the induction coil. Also, the induced healing index reduces as moisture damage increases, regardless of the heating source.

3.7. Self-healing validity equations verification

The following table (Table 8) shows the equations by which it can predict the healing index (HI) corresponding to the increase in the number of healing cycles for 20% EAFS and 0.2% SWF. To check the validity of the equations, another healing cycle was tested, and the healing index value from the laboratory test was compared to the healing index value from the equation, and the equation validity percentage was calculated as the ratio between the HI from the equation and to HI from the laboratory test. As shown in Table 9, the error between experimental and theoretical results for microwave and induction heating is approximately 1%, which means that the equations used for these calculations can be applied.

Table 7. Healing index expected equations.

Heating source	Equation	R ²
20% EAFS Induction Heating	$y = -0.018x^2 + 0.012x + 0.983$	1.000
20% EAFS Microwave Heating	$y = -0.017x^2 - 0.006x + 0.980$	0.997
0.2% SWF Induction Heating	$y = 0.004x^2 - 0.120x + 0.978$	0.999
0.2% SWF Microwave Heating	$y = 0.007x^2 - 0.146x + 1.041$	0.999

Table 8. Equations' validity and accuracy.

% of EAFS	Experimental	Theoretical	equation validity	error
20% EAFS IH	59.72%	59.30%	99.29%	0.71%
20% EAFS MH	51.95%	52.50%	101.06%	-1.06%
0.2% SWF IH	47.41%	47.80%	100.81%	-0.81%
0.2% SWF MH	48.13%	48.60%	100.98%	-0.98%

3.8. Asphalt pavement life cycle prediction (N_f & N_r)

In pavement analysis, the loads applied to the pavement surface result in two critical strains for design purposes. These critical strains are the horizontal tensile strain (ϵ_t) at the bottom of the asphalt layer and the vertical compressive strain (ϵ_v) at the top of the subgrade layer. Excessive horizontal tensile strain (ϵ_t) leads to cracking of the surface layer and fatigue-related pavement distress. On the other hand, excessive vertical compressive strain (ϵ_v) leads to permanent deformation in the pavement structure due to overloading the subgrade and causing pavement distress related to rutting. Many fatigue and rutting models have been created to establish the relationship between the asphalt modulus and the measured strains and the number of load repetitions until pavement failure. Most fatigue failure models can be represented by equation (8), while rutting models can be represented by equation (9) according to [47, 48].

$$N_f = 0.0796 * \epsilon_t^{-3.291} * E1^{-0.854} \quad (8)$$

$$N_r = 1.365 * 10^{-9} * \epsilon_v^{-4.477} \quad (9)$$

where N_f : is the number of load repetitions to prevent fatigue cracking; N_r : is the number of load repetitions to prevent rutting; ϵ_t : is the tensile strain on the bottom of the asphalt layer; ϵ_v : is the compressive vertical strain on the surface of subgrade; and $E1$ the elastic modulus of the asphalt layer. Fig. 14 illustrates the elastic modulus for CM and optimum percentages of self-healing additives: 20% EAFS and 0.2% SWF. It also shows E for the modified asphalt mixture with both 20% EAFS and 0.2% SWF. The mechanical properties and the self-healing abilities of these mixtures were provided by the authors [49]. The elastic modulus (shown in Fig.14) is determined for each damage-healing cycle from TPB test load-deformation curves as ϵ_t and ϵ_v obtained from KENPAVE software.

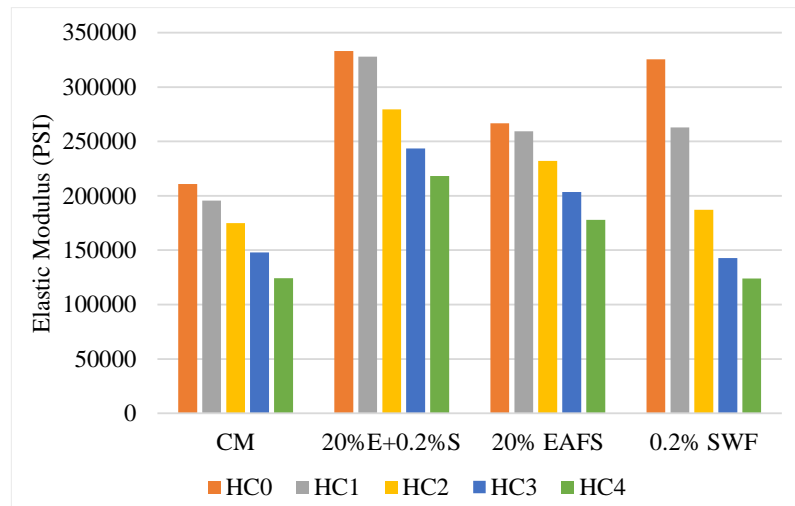


Fig. 13. CM and Modified Asphalt Mixture Elastic Modulus.

The increase in damage-healing cycle numbers led to an increase in the KENPAVE tensile strain and compressive strain, and a decrease in the number of load repetitions to prevent fatigue cracks and rutting, as shown in Figs. 15a, 16a, 15b, and 16b. 20% EAFS + 0.2 % SWF modified asphalt mixtures and 20% EAFS modified asphalt mixtures have N_f and N_r higher than CM for all healing cycles; on the other hand, 0.2% SWF modified asphalt mixtures have N_f and N_r higher than CM only at healing cycles one and two. The figures also indicate that the variation in elastic modulus significantly affects fatigue and rutting life. In comparison with the CM without any healing cycles (at healing cycle 0), modified mixtures with 20%E+0.2%S in healing cycle no.4 have N_f and N_r higher than CM by 2.2% and 5.0%, respectively.

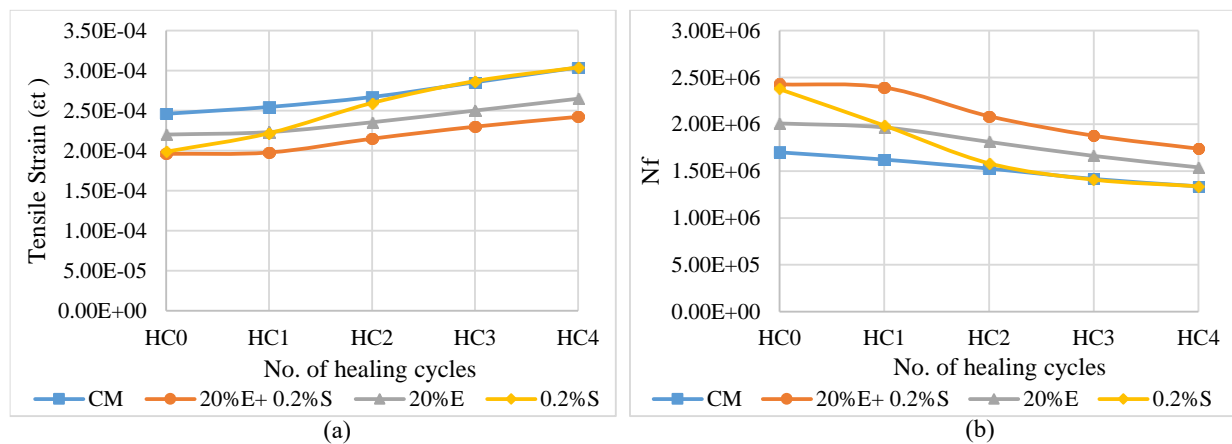


Fig. 14. (a) KENPAVE Tensile Strain, and (b) No. of Load Repetitions to Prevent Fatigue Cracking.

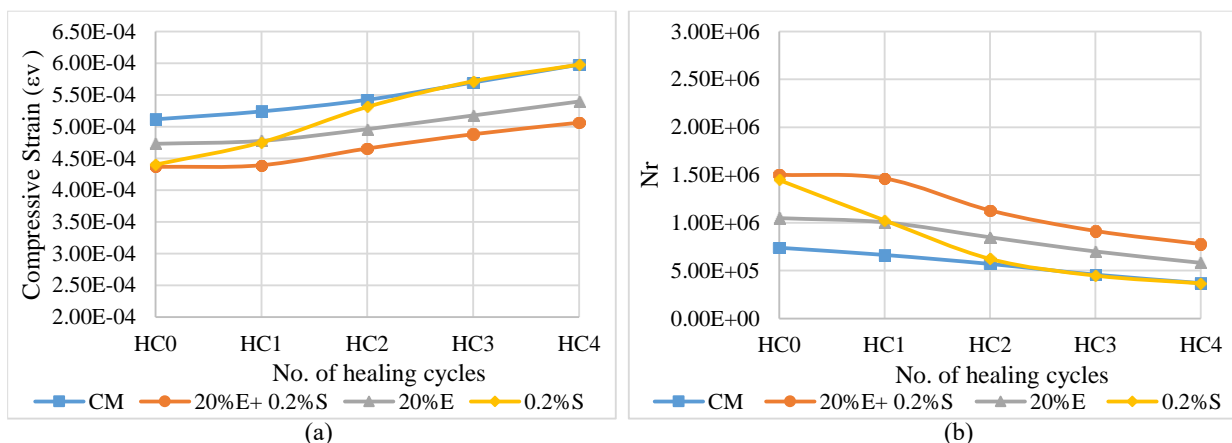


Fig. 15. (a) KENPAVE Compressive Strain, and (b) No. of Load Repetitions to Prevent Rutting.

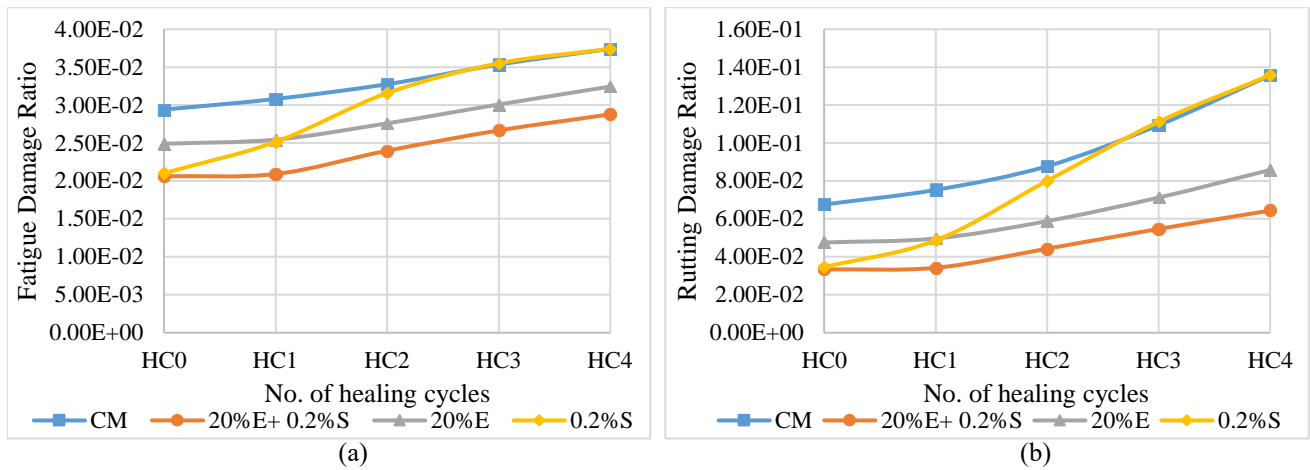


Fig. 16. Fatigue and Rutting Damage Ratio.

The fatigue and rutting damage ratios can be seen in Figs. 17a and 17b across various healing cycle numbers. These figures indicate that fatigue and rutting damage tend to rise as the healing cycle numbers increase. Also, an increase in the asphalt layer's elastic modulus leads to a reduction in fatigue and rutting damage.

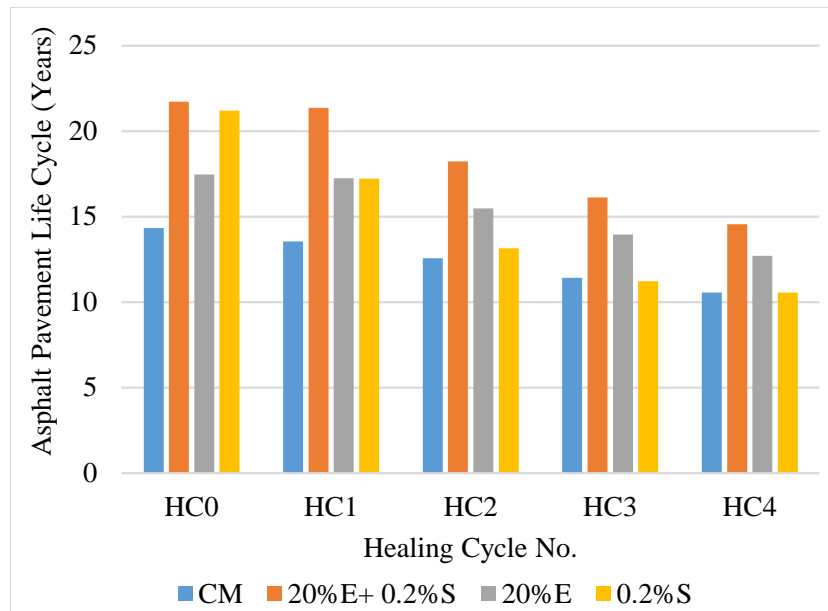


Fig. 17. Asphalt Pavement Life Cycle.

Fig. 18 illustrates the life cycle of asphalt pavement for each mixture type and the impact of increasing the number of healing cycles on pavement cycle life. As mentioned in the self-healing process section, conventional mixtures have poor self-healing capabilities, so the self-healing maintenance technique isn't used for CM for economic reasons. Based on the accumulation of cycle life for each mixture, the modified asphalt mixtures with 20% E+0.2 % S, 20% EAFS, and 0.2% SWF have life higher than CM by 47.3%, 23.1%, and 17.5%, respectively.

3.9. Cost analysis

Table 10 displays the construction cost (CC) of all asphalt mixtures used in this paper. It demonstrates that the CC of 20% EAFS Modified Asphalt Mixtures is nearly equivalent to the CM CC, while the CC of 0.2% SWF Modified Asphalt Mixtures and 20% E+0.2 % S Modified Asphalt Mixtures is only slightly higher than the CM CC by 5.5% and 4.6%, respectively. This marginal increase is insignificant when

compared to the impact of the self-healing maintenance technique on extending the lifespan of asphalt pavement. Also, concerning the impact of EAFS and SWF on increasing the elastic modulus of asphalt pavement (as depicted in Fig.14) and based on the flexible pavement design using the Empirical AASHTO 1993 method, the thickness of the surface layer decreases as the elastic modulus increases. Therefore, with or without a healing cycle, the modified asphalt mixture is more cost-effective than the conventional mixture.

Table 10. Construction Cost (CC).

Mixture Type	Conventional Mixtures	20% EAFS Modified Asphalt Mixtures	0.2% SWF Modified Asphalt Mixtures	20% EAFS+ 0.2% SWF Modified Asphalt Mixtures
Raw Materials Cost (\$/m ³)	57.5	57	61.3	60.7
Transportation and Processing (\$/m ³)			11.5	
Total cost (\$/m ³)	69	68.5	72.8	72.2

4. Conclusions

Based on the experimental program and the analysis of the results for this paper, the following conclusions are made:

- Replacement of the natural aggregate by EAF slag with a percentage range from 5% to 20% improves the mechanical properties of the asphalt mixture. The best result was obtained at 20% EAFS. Marshall stability, ITS, Fracture Toughness, and Fracture energy increased by 17.03%, 6.78%, 17.47%, and 23.29%, respectively.
- 0.2% Long SWF added to asphalt mixtures achieved the desired heating (90°C) and crack healing without a negative effect on the mechanical properties of asphalt pavement. At this percentage, the Marshall Stability decreased by 1.86% while the Marshall Quotient, ITS, Fracture Toughness, and Fracture energy increased by 3.42%, 4.44%, 9.28%, and 7.05%, respectively.
- For EAF slag, the metal element and the EAFS's higher thermal conductivity are the primary causes of the electromagnetic wave absorption and temperature increase.
- The asphalt Mixture heated by the SWF is not heated uniformly by the microwave radiation. Additionally, it was noted that SWF particles scintillated when exposed to microwave radiation. The asphalt binder around the Fibers may age as a result of this extreme heating.
- Adding large percentages of SWF to the asphalt mixture results in cluster formation and poor healing potential.
- For induction heating, the Healing index of 20% EAFS is 74.08% after four cycles of action, which is 2.36 times that of the control Mixture, and for microwave healing, it is 68.81%, which is 2.16 times that of the control Mixture.
- The crack formation affects how well an asphalt mixture heals. The crack will progressively lose its ability to heal as it becomes larger.
- 20% E+0.2 % S modified asphalt mixtures and 20% EAFS modified asphalt mixtures consistently exhibit higher Nf and Nr values than CM for all healing cycles. Conversely, 0.2% SWF-modified asphalt mixtures only demonstrate higher Nf and Nr values than CM in the first two healing cycles.
- The increase in asphalt pavement life cycle for 0.2%SWF was 17.5% For with a 5.6% increase in construction cost, then 23.1% for 20%EAFS with no increase in CC, then 47.3% for 20%E+0.2%S with a 4.9% increase in CC. This indicates the development of an environmentally sustainable asphalt mixture with a decrease in the amount of natural resources and a solution to landfill disposal.

Future work

- Investigate the combined effect of adding encapsulating bitumen solvent with EAFS or SWF or both to enhance healing efficiency, reduce energy consumption, and extend the pavement life cycle.
- Evaluate the impact of long-term aging on EAFS and SWF-modified asphalt mixtures under various aging conditions, including oxidative aging and UV exposure, to better understand the durability of these mixtures over time.
- The effectiveness of self-healing properties using induction and microwave heating should be validated through real roads.

Funding

This research did not receive any specific grant from funding agencies in the public, commercial, or not-for-profit sectors.

Conflicts of interest

The authors declare that they have no known competing financial interests or personal relationships that could have appeared to influence the work reported in this paper.

Authors contribution statement

Catherine Gamil Shafik: Conceptualization; Methodology; Software; Writing - Original Draft; Data Curation.

Dr. Mohamed R. Elshahat: Supervision; Methodology; Investigation; Writing - Review & Editing.

Dr. Ahmed Abdelghani Mahmoud: Supervision; Data Curation; Visualization; Writing - Review & Editing.

Prof. Abdelzaher E. A. Mostafa: Supervision; Conceptualization; Methodology; Resources; Formal analysis; Validation; Writing - Review & Editing.

References

- [1] Lou B, Sha A, Li Y, Wang W, Liu Z, Jiang W, et al. Effect of metallic-waste aggregates on microwave self-healing performances of asphalt mixtures. *Constr Build Mater* 2020;246:118510. <https://doi.org/10.1016/j.conbuildmat.2020.118510>.
- [2] Jwaida Z, Dulaimi A, Mydin MAO, Özkılıç YO, Jaya RP, Ameen A. The Use of Waste Polymers in Asphalt Mixtures: Bibliometric Analysis and Systematic Review. *J Compos Sci* 2023;7. <https://doi.org/10.3390/jcs7100415>.
- [3] Khan MA, Khan MS, Nasir B, Khan A, Sabri MMS, Ahmad M, et al. Performance optimization of asphalt pavements using binder film thickness as a criterion in innovative mix design compared to Marshall and Superpave methods. *Front Mater* 2024;11:1–18. <https://doi.org/10.3389/fmats.2024.1488310>.
- [4] Garcia A, Salih S, Gómez-meijide B. Optimum moment to heal cracks in asphalt roads by means electromagnetic induction. *Constr Build Mater* 2020;238:117627. <https://doi.org/10.1016/j.conbuildmat.2019.117627>.
- [5] Abdelghani Mahmoud A, Fouad M, E. A. Mostafa A. Evaluation of Self-Healing Performance of the Hot Mix Asphalt Using Metallic Wool and Recycled Materials. *Eng Res J* 2022;175:1–18. <https://doi.org/10.21608/erj.2022.258131>.
- [6] Salih SI. Self-Healing of cycle loading damage in asphalt mixtures. The university of Nottingham, 2020.

- [7] Mostafa AEA, Ouf MS, Abdel Fatah HH. Evaluation of Using Waste Road Construction Materials with Additives in Warm Mix Asphalt. *Sustain Civ Infrastructures* 2018;322–34. https://doi.org/10.1007/978-3-319-61633-9_22.
- [8] Eloufy AM, Mostafa AEA, Ouf MS, Ibrahim MF. Evaluating the Performance of Half Warm Asphalt Mixtures Using Reclaimed Asphalt Pavement (RAP). *PORT SAID Eng Res J* 2022;62:56–63. <https://doi.org/10.21608/PSERJ.2022.135558.1185>.
- [9] Eloufy AM, Mostafa AEA, Ouf MS, Ibrahim MF. Investigating the Engineering Properties of Half-Warm Asphalt Mixes Using Chemical Additives. *Egypt Int J Eng Sci Technol* 2022;40:61–70. <https://doi.org/10.21608/eijest.2022.125423.1141>.
- [10] Nasser AM, Abd El-Wahab H, Abd El-Fattah M, Mostafa AEA, Sakr AG. Preparation and characterization of modified reclaimed asphalt by using styrene – Butyl acrylate nanoemulsioncopolymer. *Egypt J Chem* 2018;61:269–380. <https://doi.org/10.21608/ejchem.2018.2956.1245>.
- [11] Nasser AM, El-wahab HA, El-fattah MA, Mostafa AEA, Sakr G. Study on Modification of Reclaimed Asphalt Pavements By Using Some Acrylate Polymers. *Al-Azhar Bull Sci* 2017;28:31–41. <https://doi.org/10.21608/absb.2017.8108>.
- [12] Radeef HR, Abdul Hassan N, Mahmud MZH, Zainal Abidin AR, Ismail CR, Abbas HF, et al. Characterisation of cracking resistance in modified hot mix asphalt under repeated loading using digital image analysis. *Theor Appl Fract Mech* 2021;116:103130. <https://doi.org/10.1016/j.tafmec.2021.103130>.
- [13] Mirabdolazimi SM, Kargari AH, Pakenari MM. New achievement in moisture sensitivity of nano-silica modified asphalt mixture with a combined effect of bitumen type and traffic condition. *Int J Pavement Res Technol* 2021;14:105–15. <https://doi.org/https://doi.org/10.1007/s42947-020-0043-y>.
- [14] Mostafa AEA, Tawhed WMF, Elshahat MR, Sherif AG. Developing New Design Criteria of Asphalt Pavement Mix Using Nano-Materials and Polymer-Materials. *Int J Adv Eng Nano Technol* 2018;335–47. https://doi.org/10.1007/978-3-319-61633-9_23.
- [15] Naser AM, Abd El - Wahab H, Moustafa El Nady MAEF, E. A. Mostafa A, Lin L, Sakr AG. Preparation and characterisation of modified reclaimed asphalt using nanoemulsion acrylate terpolymer. *Pigment Resin Technol* 2019;48:363–74. <https://doi.org/10.1108/PRT-08-2018-0080>.
- [16] Afshin A, Behnood A. Nanomaterials in asphalt pavements: A state-of-the-art review. *Clean Waste Syst* 2025;10:100214. <https://doi.org/10.1016/j.clwas.2025.100214>.
- [17] Kumar H, Varma S. A review on utilization of steel slag in hot mix asphalt. *Int J Pavement Res Technol* 2021;14:232–42. <https://doi.org/10.1007/s42947-020-0025-0>.
- [18] Hassan HF, Al-Shamsi K, Al-Jabri K. Effect of Steel Slag on the Permanent Deformation and Life Cycle Cost of Asphalt Concrete Pavements. *Int J Pavement Res Technol* 2023. <https://doi.org/10.1007/s42947-023-00314-x>.
- [19] Zhang R, Zhang W, Shen S, Wu S, Zhang Y. Evaluation of the correlations between laboratory measured material properties with field cracking performance for asphalt pavement. *Constr Build Mater* 2021;301:124126. <https://doi.org/10.1016/j.conbuildmat.2021.124126>.
- [20] Liu J, Yang X, Lau S, Wang X, Luo S, Lee VC-S, et al. Automated pavement crack detection and segmentation based on two-step convolutional. *Comput Aided Civ Eng* 2020. <https://doi.org/10.1111/mice.12622>.
- [21] Yamaç ÖE, Yilmaz M, Yalçın E, Kök BV, Norambuena-Contreras J, Garcia A. Self-healing of asphalt mastic using capsules containing waste oils. *Constr Build Mater* 2021;270. <https://doi.org/10.1016/j.conbuildmat.2020.121417>.
- [22] Sun X, Qin X, Liu Z, Yin Y, Zou C, Jiang S. New preparation method of bitumen samples for UV aging behavior investigation. *Constr Build Mater* 2020;233:117278. <https://doi.org/10.1016/j.conbuildmat.2019.117278>.
- [23] Zhang H, Chen Z, Xu G, Shi C. Evaluation of aging behaviors of asphalt binders through different rheological indices. *Fuel* 2018;221:78–88. <https://doi.org/10.1016/j.fuel.2018.02.087>.
- [24] Franesqui MA, Yepes J, García-González C. Top-down cracking self-healing of asphalt pavements with steel filler from industrial waste applying microwaves. *Constr Build Mater* 2017;149:612–20. <https://doi.org/10.1016/j.conbuildmat.2017.05.161>.

- [25] Behnia B, Reis H. Self-healing of thermal cracks in asphalt pavements. *Constr Build Mater* 2019;218:316–22. <https://doi.org/10.1016/j.conbuildmat.2019.05.095>.
- [26] Jwaida Z, Dulaimi A, Othuman A, Yasir M, Shakir NK, Busaltan A. The self - healing performance of asphalt binder and mixtures: a state - of - the - art review. Springer International Publishing; 2024. <https://doi.org/10.1007/s41062-024-01547-w>.
- [27] Grossegger D, Garcia A. Influence of the thermal expansion of bitumen on asphalt self-healing. *Appl Therm Eng* 2019;156:23–33. <https://doi.org/10.1016/j.applthermaleng.2019.04.034>.
- [28] Grossegger D, Gomez-Meijide B, Vansteenkiste S, Garcia A. Influence of rheological and physical bitumen properties on heat-induced self-healing of asphalt mastic beams. *Constr Build Mater* 2018;182:298–308. <https://doi.org/10.1016/j.conbuildmat.2018.06.148>.
- [29] Xu Z, Xu T. Improving Effects of Pretreated Graphene on Pavement Performance and Self-Healing Behaviors of Asphalt Mixture. *Int J Pavement Res Technol* 2023. <https://doi.org/10.1007/s42947-023-00401-z>.
- [30] Moharam O, Mostafa A. Improving life cycle of asphalt pavement mixture using Self-Healing Techique. *J Int Soc Sci Eng* 2023;0:0–0. <https://doi.org/10.21608/jisse.2023.209844.1074>.
- [31] Ruiz-Riancho N, Garcia A, Grossegger D, Saadoon T, Hudson-Griffiths R. Properties of Ca-alginate capsules to maximise asphalt self-healing properties. *Constr Build Mater* 2021;284:122728. <https://doi.org/10.1016/j.conbuildmat.2021.122728>.
- [32] Norambuena-Contreras J, Garcia A. Self-healing of asphalt mixture by microwave and induction heating. *Mater Des* 2016;106:404–14. <https://doi.org/10.1016/j.matdes.2016.05.095>.
- [33] Jeoffroy E, Bouville F, Bueno M, Studart AR, Partl MN. Iron-based particles for the magnetically-triggered crack healing of bituminous materials. *Constr Build Mater* 2018;164:775–82. <https://doi.org/10.1016/j.conbuildmat.2017.12.223>.
- [34] Pérez I, Gómez-Meijide B, Pasandín AR, García A, Airey G. Enhancement of curing properties of cold in-place recycling asphalt mixtures by induction heating. *Int J Pavement Eng* 2019;22:355–68. <https://doi.org/10.1080/10298436.2019.1609674>.
- [35] Kargari A, Arabani M, Mirabdolazimi SM. Effect of palm oil capsules on the self-healing properties of aged and unaged asphalt mixtures gained by resting period and microwave heating. *Constr Build Mater* 2022;316:125901. <https://doi.org/10.1016/j.conbuildmat.2021.125901>.
- [36] Anupam BR, Sahoo UC, Chandrappa AK. A methodological review on self-healing asphalt pavements. *Constr Build Mater* 2022;321:126395. <https://doi.org/10.1016/J.CONBUILDMAT.2022.126395>.
- [37] Abbad El Andaloussi N, Zaoui A. Enhancing Mechanical and Self-Healing Properties of Asphalt Binder Through the Incorporation of Nano-silica. *Int J Pavement Res Technol* 2023;16:1–14. <https://doi.org/10.1007/s42947-021-00105-2>.
- [38] Fan S, Wang H, Zhu H, Sun W. Evaluation of Self-Healing Performance of Asphalt Concrete for Low-Temperature Fracture Using Semicircular Bending Test. *J Mater Civ Eng* 2018;30:1–8. [https://doi.org/10.1061/\(asce\)mt.1943-5533.0002426](https://doi.org/10.1061/(asce)mt.1943-5533.0002426).
- [39] Phan TM, Park DW, Le THM. Crack healing performance of hot mix asphalt containing steel slag by microwaves heating. *Constr Build Mater* 2018;180:503–11. <https://doi.org/10.1016/j.conbuildmat.2018.05.278>.
- [40] Sun Y, Wu S, Liu Q, Zeng W, Chen Z, Ye Q, et al. Self-healing performance of asphalt mixtures through heating fibers or aggregate. *Constr Build Mater* 2017;150:673–80. <https://doi.org/10.1016/j.conbuildmat.2017.06.007>.
- [41] Yang H, Ouyang J, Jiang Z, Ou J. Effect of fiber reinforcement on self-healing ability of asphalt mixture induced by microwave heating. *Constr Build Mater* 2023;362:129701. <https://doi.org/10.1016/j.conbuildmat.2022.129701>.
- [42] Norambuena-Contreras J, Garcia A. Crack-healing evaluation of fibre-reinforced asphalt mixtures using microwave and induction heating. *Road Mater Pavement Des* 2017;0:1–11. <https://doi.org/10.1080/14680629.2017.1304267>.
- [43] Gao J, Sha A, Wang Z, Tong Z, Liu Z. Utilization of steel slag as aggregate in asphalt mixtures for microwave deicing. *J Clean Prod* 2017;152:429–42. <https://doi.org/10.1016/j.jclepro.2017.03.113>.

- [44] Liu J, Wang Z, Jing H, Zhang T, Wang X, Zhou X, et al. Self-healing properties of steel slag asphalt mixture based on experimental characterization and 3D reconstruction. *Mater Des* 2023;234. <https://doi.org/10.1016/j.matdes.2023.112358>.
- [45] García A, Norambuena-Contreras J, Bueno M, Partl MN. Influence of steel wool fibers on the mechanical, thermal, and healing properties of dense asphalt concrete. *J Test Eval* 2014;42. <https://doi.org/10.1520/JTE20130197>.
- [46] Norambuena-Contreras J, Serpell R, Valdés Vidal G, González A, Schlangen E. Effect of fibres addition on the physical and mechanical properties of asphalt mixtures with crack-healing purposes by microwave radiation. *Constr Build Mater* 2016;127:369–82. <https://doi.org/10.1016/j.conbuildmat.2016.10.005>.
- [47] Karimi MM, Darabi MK, Jahanbakhsh H, Jahangiri B, Rushing JF. Effect of steel wool fibers on mechanical and induction heating response of conductive asphalt concrete. *Int J Pavement Eng* 2020;21:1755–68. <https://doi.org/10.1080/10298436.2019.1567918>.
- [48] Liu J, Zhang T, Guo H, Wang Z, Wang X. Evaluation of self-healing properties of asphalt mixture containing steel slag under microwave heating: Mechanical, thermal transfer and voids microstructural characteristics. *J Clean Prod* 2022;342:130932. <https://doi.org/10.1016/j.jclepro.2022.130932>.
- [49] Mahmoud AA, Shafik CG, Elshahat MR, Mostafa AEA. Producing Self-Healing Asphalt Pavement Mixture using Induction and Microwave Heating. *Trends Adv Sci Technol* 2024;1. <https://doi.org/10.62537/2974-444x.1010>.
- [50] Shiha M, El-Badawy S, Gabr A. Modeling and performance evaluation of asphalt mixtures and aggregate bases containing steel slag. *Constr Build Mater* 2020;248:118710. <https://doi.org/10.1016/j.conbuildmat.2020.118710>.
- [51] Hassan KE, Attia MIE, Reid M, Al-Kuwari MBS. Performance of steel slag aggregate in asphalt mixtures in a hot desert climate. *Case Stud Constr Mater* 2021;14:e00534. <https://doi.org/10.1016/j.cscm.2021.e00534>.
- [52] Ayatollahi MR, Mahdavi E, Alborzi MJ, Obara Y. Stress intensity factors of semi-circular bend specimens with straight-through and chevron notches. *Rock Mech Rock Eng* 2016;49:1161–72. <https://doi.org/10.1007/s00603-015-0830-y>.
- [53] Rind TA, Jhatial AA, Sandhu AR, Bhatti IA, Ahmed S. Fatigue and Rutting Analysis of Asphaltic Pavement Using “KENLAYER” Software. *J Appl Eng Sci* 2019;9:177–82. <https://doi.org/10.2478/jaes-2019-0024>.
- [54] Behiry AEAEM. Fatigue and rutting lives in flexible pavement. *Ain Shams Eng J* 2012;3:367–74. <https://doi.org/10.1016/j.asej.2012.04.008>.